FULL PAPER

Droplet Manipulation

ADVANCED
MATERIALS
INTERFACES
www.advmatinterfaces.de

Directed Pinning of Moving Water Droplets on Photoresponsive Liquid Crystal Mats

Yuyun Liu, Chongyu Zhu, Yong Zhao, Xin Qing, Feng Wang, Daosheng Deng, Jia Wei, and Yanlei Yu*

Compared to conventional continuous-flow liquid manipulation, the direct control of liquid droplets on an open surface prevents the potential cross contamination during liquid transfer, which is advantageous for biological microliquids. However, the fabrication techniques of smart surfaces and the fast manipulation of droplets remotely remain difficult, limiting its practical application. Herein, large-scaled photoresponsive superhydrophobic mats fabricated by the electrospinning of linear liquid crystal polymer are presented. Upon the alternated irradiation of UV–vis light, these mats exhibit significant, fast, and reversible change of adhesion, while their surfaces maintain the superhydrophobicity. Therefore, the water droplets can be pinned at any directed point on the mat surface after the fast superhydrophobic adhesion switch by the remote control of light. It is expected that the active manipulation of discrete droplets on an open surface through these photoresponsive mats provides a new concept for microdroplet manipulation, allowing for minimal reactions among biological samples.

1. Introduction

Manipulating droplets on solid surfaces showed potentials in a wide range of applications, from bioinspired liquid transfer to lab-on-a-chip devices. Instead of using continuous flow, direct control of discrete droplets is sometimes preferred in microfluidic devices as it minimizes the cross contamination between droplets, allowing for small-volume biological sample analysis.[1,2] So far, several approaches, including the usage of electrowetting defects and the magnetic force, have successfully demonstrated the manipulation of droplets on an open surface. However, the high operating voltages and/or the responsive additives used in these systems limit their application in biological fields.[3–9] Compared to other stimuli, light allows a precise and remote control that can be regulated by tunable intensities and wavelengths, providing an alternative tool for the liquid manipulation.[6–12] For example, Ichimura et al. achieved the remote light manipulation of liquids on an open surface modified with a photoresponsive azobenzene monolayer.[9] The azobenzene mesogens underwent *trans* to *cis* isomerization upon light irradiation, varying the surface tension of the droplet on one side, therefore drove the droplets toward the desired direction. However, the lyophilicity property of the modified surface makes it unsuitable for the control of water, the most commonly used liquid in biological fields.

Surperhydrophobic surfaces have been suggested as a desirable candidate for the manipulation of water droplets. With the aid of photoresponsive materials, people have managed to tune the water contact angle (CA) on various superhydrophobic surfaces with photoresponsive nano-/microstructures such as microarrayed surfaces[13,14] by the light irradiation. However, the dynamic control of water droplets remains difficult in these systems due to the unchanged adhesion from these surfaces. Among all the photoresponsive materials, azobenzene-containing liquid crystal polymers (LCPs) showed superior in the manufacture of the photoresponsive superhydrophobic surfaces.[14–17] Owing to the photoinduced orientation change caused by *trans*/*cis* isomerization of azobenzene along with the cooperative effect of the liquid crystals (LCs), these polymers are able to produce large, rapid, and reversible deformation or surface free energy changes in response to light, which is ideal for tuning the physical and chemical properties of the nano-/microstructures on the surfaces for water manipulation.[18–26] The quick and reversible switch of superhydrophobic adhesion has been demonstrated on a microarrayed crosslinked LCP film, which was fabricated by polydimethylsiloxane soft template–based secondary replication.[14] However, the complex technique results in the difficulties in modulation of micro-/nanostructure and the size of the prepared surface with hierarchical structure is limited at square millimeter scale.

Dr. Y. Y. Liu, Dr. C. Y. Zhu, Dr. X. Qing, Dr. J. Wei, Prof. Y. L. Yu
Department of Materials Science and State Key Laboratory of Molecular Engineering of Polymers
Fudan University
Shanghai 200433, P. R. China
E-mail: ylyu@fudan.edu.cn
Prof. Y. Zhao
Key Laboratory of Bioinspired Smart Interfacial Science and Technology of Ministry of Education
Beijing Key Laboratory of Bioinspired Energy Materials and Devices
School of Chemistry and Environment
Beihang University
Beijing 100191, P. R. China
F. Wang, Prof. D. S. Deng
Department of Aeronautics and Astronautics
Fudan University
Shanghai 200433, P. R. China

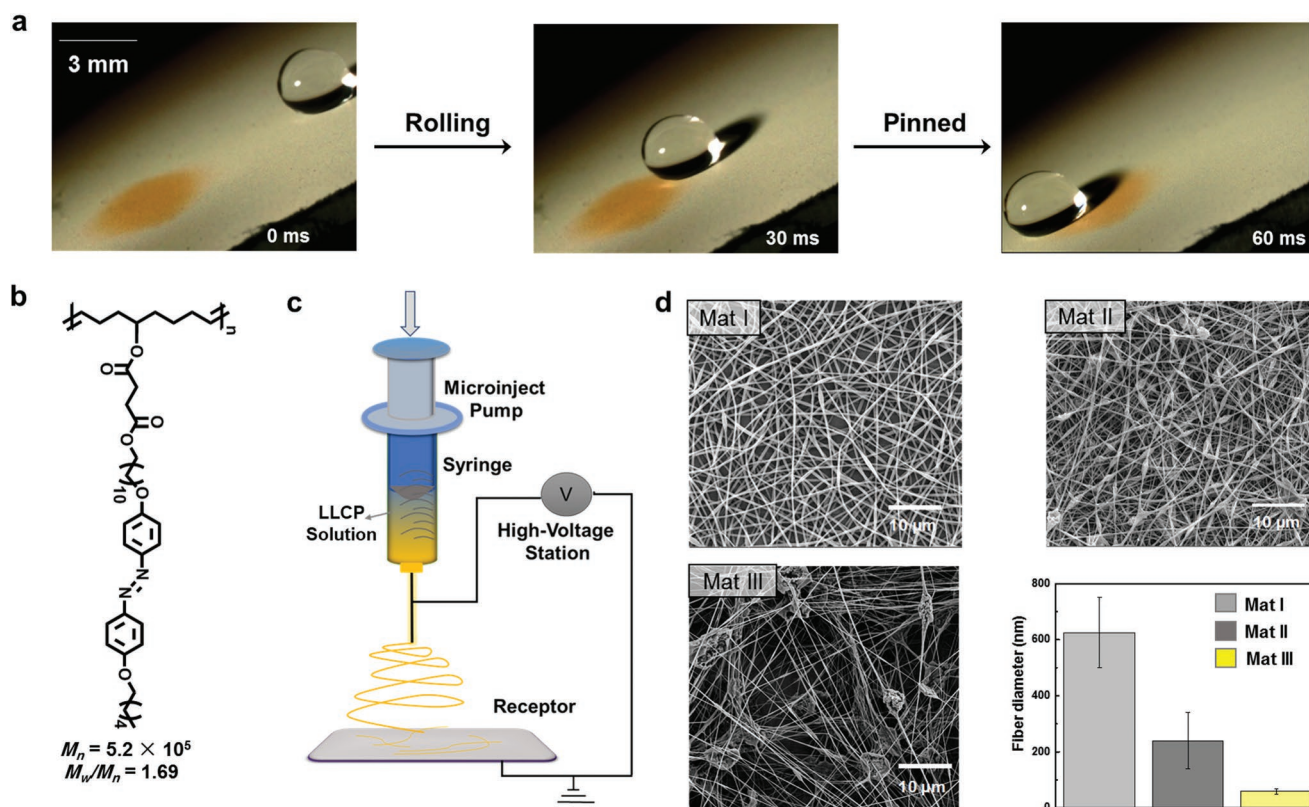**Figure 1.** a) Screenshots from high-speed video of pinning moving water droplet. The orange area was irradiated by UV light (365 nm, 20 mW cm^{-2}, 2 s). b) Molecular structure of a linear liquid crystal polymer (LLCP). M_n, number-average molecular weight; M_w, weight-average molecular weight. c) Schematic view of the electrospinning processing. d) Representative FESEM image of the nanofiber Mats I–III and quantification of fiber diameters in Mats I–III. All the fibers are continuous and randomly oriented. In an effort to obtain the superhydrophobic surface with low adhesive force (AF), the film morphology was regulated and controlled by adjusting concentration of solutions.

Electrospinning, on the contrary, has shown its application in directly and continuously fabricating superhydrophobic nanofiber mats with unique surface roughness and texture in a large scale.[27] Yet, it is not compatible to the photoresponsive crosslinked LCPs, the current materials that guarantee enough mechanical support for significant surface morphology and properties change. Moreover, the existing linear azo-LCPs with low molecular weight are difficult to be constructed into fibers through the unstable jetting process during electrospinning.[28–33] Recently, our group developed a high molecular weight linear LCP (LLCP) containing azobenzene units, with which we managed to fabricate a 3D microtube exhibiting excellent photodeformability. Owing to its good mechanical properties and processing performance, this polymer is an ideal material for the construction of photoresponsive mats by electrospinning.[7]

Herein, based on the photoresponsive LLCP with high molecular weight, we first construct photoresponsive superhydrophobic mats in a large scale by electrospinning and demonstrate the fast switch of superhydrophobic adhesion of the mats controlled by light. The rapid and large changes of adhesive force (AF) and the surface free energy on the mats arise from the polarity change and the reorientation of photoisomerized azobenzene mesogens on the surface of nanofibers. Possessing this unique photoresponsive property, these mats allow the pinning of the water droplets at any directed point on the surface after UV light irradiation for 2 s (**Figure 1**a). The novel photoresponsive LLCP mat is an ideal candidate to achieve the active manipulation of discrete droplets on an open surface, which will enable the further extension of minimum bioreaction for diagnostics and drug screening.

2. Results and Discussion

2.1. Fabrication of the Superhydrophobic LLCP Mats

To obtain the superhydrophobic LLCP mats, a high number-average molecular weight (5.2×10^5 g mol^{-1}) azobenzene-containing LLCP[7] (Figure 1b) solution in dichloromethane was processed into nanofiber mats by electrospinning. As concentration plays a major role in electrospinning and has a significant influence on the morphology of fabricated mat,[25] three mats were prepared by altering the solution concentration from 5, 3 to 1 wt% (Figure 1c). As shown in Figure 1d, with the decrease of LLCP concentration, the diameter of the fibers in Mats I–III decreased from 625 ± 120 to 63 ± 10 nm and the morphologies of the surface varied from fiber (Mat I) to fiber interconnected by particles (Mat II and Mat III). As wettability is directly affected by the roughness of surface, the water

**ADVANCED
SCIENCE NEWS**
www.advancedsciencenews.com

**ADVANCED
MATERIALS
INTERFACES**
www.advmatinterfaces.de

CAs and sliding angels (SAs) of these mats were measured, illustrated in Table S1 (Supporting Information). Compared to the flat LLCP surface (Figure S1, Supporting Information), the CAs of Mats I–III increase greatly with the introduction of surface roughness. In this study, a lower concentration gave a larger roughness, a bigger CA, and a lower SA for the mat. The CA of Mats I–III increased from 135.4° to 150.0°. Mats I and II showed high adhesion, which could pin a droplet even if it is hung upside down. Mat III was a superhydrophobic mat possessing a CA of 150.9° ± 0.9° and a SA of 20° ± 0.5°.

2.2. Photoresponsive Wettability and Adhesion of LLCP Films

Photoresponse of the LLCP was confirmed by UV–vis spectroscopy (Figure S2, Supporting Information). The changes of the absorption bands suggest that the LLCP molecules possess photoisomerization behavior from *trans* to *cis* isomers under UV light irradiation, which gives rise to a change in dipole moment. To discern whether the photoresponsibility of azobenzene is retained in the electrospinning mat, the results of CAs of Mat III were recorded with an alternating irradiation of UV and visible light (Figure S3, Supporting Information). The *trans/cis* isomerization of azobenzene on the surface of nanofibers results in the increase of surface energy and the decrease of CA owing to the higher dipole presented in the *cis* isomer than in the *trans* isomer. In particular, the CA of Mat III changed slightly from 150.1° ± 0.7° to 147.2° ± 1.2° after UV light irradiation (365 nm, 20 mW cm⁻², 2 s) and recovered back after visible light irradiation (530 nm, 60 mW cm⁻², 20 s), holding a superhydrophobic state that is ideal for further liquid manipulation.

Upon UV, the SA showed no changes in Mats I and II while Mat III showed a phototunable superhydrophobic adhesion and obvious change of SA. Compared with the initial low adhesive state, the AFs of Mat III were enlarged by 100% after UV light irradiation (365 nm, 20 mW cm⁻², 2 s) (**Figure 2**a). Moreover, the AFs of UV-irradiated area were large enough to pin an 8 µL water droplet hanging from above (Figure S4a, Supporting Information). Upon visible light irradiation (530 nm, 60 mW cm⁻², 20 s), AFs recovered and thus the 8 µL water droplet could roll off from the surface when the substrate was tilted above 20° (Figure S4b, Supporting Information). This photoresponsive wettability was demonstrated to be reversible for a few cycles. Previous reported azobenzene-containing polymer mats[13] only showed the wettability change after long time of light irradiation (at least 1 h). In our work, this LLCP mat not only shows superhydrophobic wettability change but also significantly fast adhesion transition (within 2 s).

2.3. Directed Pinning of Moving Water Droplets

This fast switch of superhydrophobic adhesion is a considerable benefit for the active manipulation of liquid droplets. The directed pinning of moving water droplets is successfully achieved on the inclined LLCP mat (Movies S1 and S2, Supporting Information). Figure 2d shows a series of snapshots of water droplets (8 µL) sliding down the inclined surface upon

different light irradiations. In the initial state, the water droplets roll down the inclined superhydrophobic surface with a slant angle of 20° (Movie S3, Supporting Information). After UV light irradiation, the moving water droplets are pinned by the exposed area (365 nm, 20 mW cm⁻², 2 s) due to the increased AFs. It is obvious that the irradiated point turns from yellow to orange upon UV irradiation owing to the absorbance of the *cis* isomer of azobenzene. After removing the pinned droplets and irradiated by visible light (530 nm, 60 mW cm⁻², 20 s), the irradiated area returns to a low adhesion state and thus the new droplets could roll down again (Figure 2d-VI). Superior to trapping of droplets based on electrically wetting defect[3] or magnetic, this mat allows free and remote control of pinning droplets at any irradiated position without contamination, providing opportunity for the no-loss manipulation of biological microsamples on the open surface (Figures S8 and S9, Supporting Information).

Thanks to the advantages of light as the stimulus and the superhydrophobic mats with large area, we also achieved precise control of the droplet array on the mats which facilitate integrated control of microdroplets on an open surface in the future. As shown in **Figure 3**a, we fabricated patterns of adhesion regions on a single mat by using UV light irradiation through various masks. After UV irradiation, the selectively exposed regions become of high adhesion and the masked areas maintain their low adhesion properties. Diverse shapes were obtained on one same mat upon alternated irradiation by UV and visible light, such as "FD" shape, heart shape, and "LC" shape (Figure 3b). Moreover, upon visible light illumination, the water adhesion patterns vanish and the mat recovers to its initial low adhesion state, which indicates that it is easy to create the erasable and rewritable photoresponsive patterned substrates by using LLCP mats with switchable water adhesion properties.

2.4. Critical Conditions for Pinning Water Droplets

In order to calculate the critical conditions for pinning water droplets on mats irradiated by different light (UV–vis), we assume that there is no contact angle hysteresis for a droplet rolling on an inclined surface according to the rolling model for rough surface.[34] The relationship between the slant angle α and the volume of water droplet V follows the formula

$$\sin\alpha \approx kV^{-2/3} \tag{1}$$

k is a coefficient related to the properties of the mat surface after irradiated by light with different wavelengths. We take the data of Table S2 (Supporting Information) into the formula (1) and obtain the relationship between $\sin\alpha$ and V in different conditions by proper fitting of the experimental data (Figure 2b and Figure S5 (Supporting Information)): before UV irradiation or after visible light irradiation, $\sin\alpha = 0.9V^{-2/3}$; after UV irradiation, $\sin\alpha = 1.6V^{-2/3}$. When irradiated by different lights (UV–vis), the roughness factor and the chemical property may change, leading to the change of the coefficient k, which is the foundation for the active manipulation of the droplets on the LLCP mat. When the values of $\sin\alpha$ and V belong to the "switch region" which is under the red line and
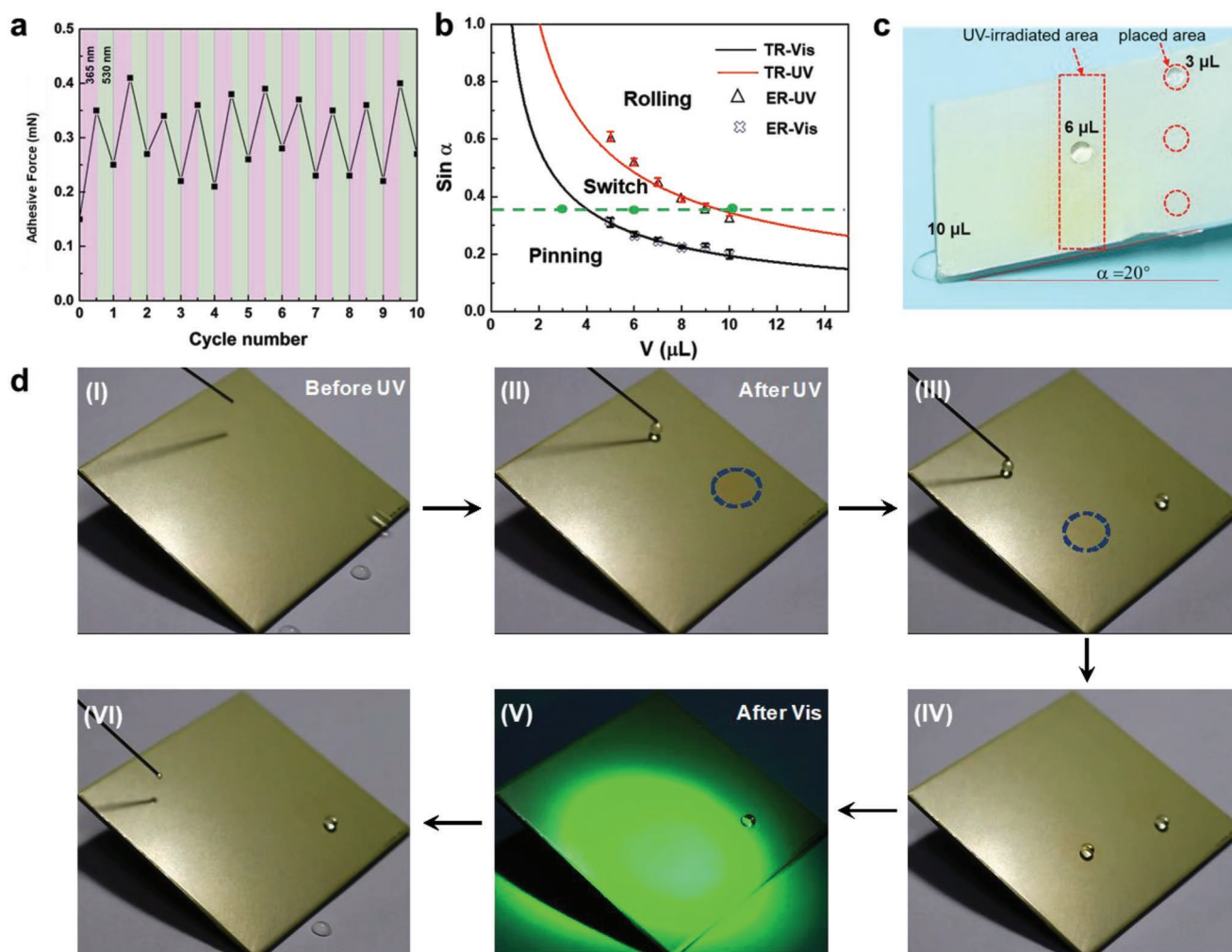
Figure 2. a) AF results with alternating UV–vis irradiation (ten cycles). Upon UV irradiation for 2 s, the AF increase double. After visible light irradiation for 20 s, the AFs recover. b) Plots of theoretical results (TRs) and experimental results (ERs) of the critical conditions for pinning water droplets on mats irradiated by different lights (UV–vis). c) Screening droplets with different volumes. Three water droplets are placed on the slant mat ($\alpha = 20°$) with middle area irradiated by UV light. The 3 µL droplet is stuck on the unirradiated part, while the 10 µL droplet rolls off the mat, the 6 µL droplet rolls and is pinned at the irradiated position. d) Photographs of directed pinning of moving water droplets on superhydrophobic mat: I) 8 µL water droplets rolling down the surface of the mat; II–IV) the circled areas are shined by UV light, turning orange owing to the photoisomerization of azobenzene units. Then, the moving droplets could be pinned at the UV-irradiated points; V,VI) the mat returns to a low AF state after visible light irradiation and the droplets slid down smoothly. UV light: 365 nm, 20 mW cm^{-2}; visible light: 530 nm, 60 mW cm^{-2}; size of the mat: 5.0 cm × 5.0 cm.

above the black line, the water droplet can roll down before UV irradiation but pinned after UV irradiation on the photoresponsive mat surface. The theoretical results and experimental measurements coincide very well. Having a better understanding of the critical conditions for pinning water droplets, we then used these photoresponsive mats for water droplet separation. As shown in Figure 2c, three water droplets with different volumes (3, 6, and 10 µL) were added onto a photoresponsive mat with middle area irradiated by UV light, which was placed at an inclination angle of 20°. The small-volume (3 µL) droplet was stuck on the unirradiated part of the mat while the large-volume (10 µL) droplet rolled off the mat. Only the droplet of 6 µL was rolling and pinned at the irradiated position, which fits the data (the three points on the dashed line) from Figure 2b.

2.5. Reasons for Adhesion Change of LLCP Mats

The polarity change of azobenzene induced by UV light gives rise to an increase of the free energy and the AF of the surface (Figure 2a and Figure S3 (Supporting Information)).[12,33] We anticipate that the LC order in the LLCP nanofiber mats also plays an important role in the fast change of wettability and adhesion. The 2D wide-angle X-ray diffraction (WAXD) pattern shows that the nanofiber mats possess a LC semetic phase at room temperature (Figure S6, Supporting Information). The mesomorphic properties of the aligned nanofibers were further evaluated by tracing their transmittance between two crossed polarizers at room temperature. The highest transmittance occurred at an angle of 45° between the polarization direction of either polarizer and the axial direction of the nanofibers
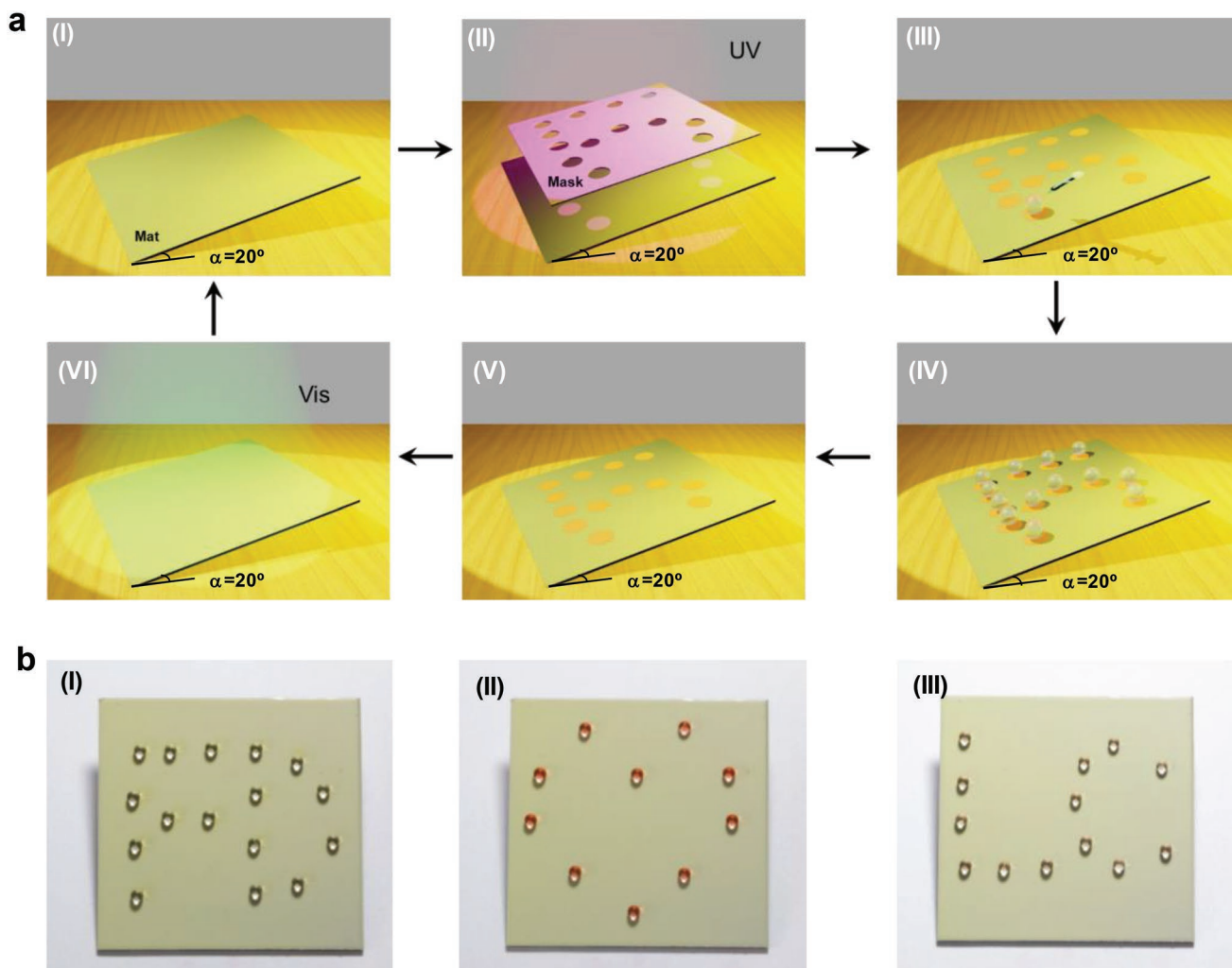
Figure 3. a) Schematic diagrams of the reusable adhesion pattern on the superhydrophobic mat: I) before UV light irradiation; II,III) after exposure with UV light (365 nm, 20 mW cm^{-2}, 2 s) through a LC-shaped photomask, then the irradiated areas switch from yellow to orange possessing a higher AF compared with the unexposed area; IV,V) the water droplets are able to be pinned at the UV-irradiated position to form "LC" shape; VI) after exposure with visible light (530 nm, 60 mW cm^{-2}, 20 s), the mat recovers to the original state with low adhesion. b) Photographs of mats with patterned wetting properties: I) "FD" shape; II) heart shape; III) "LC" shape. Size of the mat: 5.0 cm × 5.0 cm.

(**Figure 4**a). Whereas, the lowest transmittance appeared when the polarization direction was parallel to the long axis direction of the fibers. This result reveals that the mesogens are well oriented parallel to the long axis of the nanofibers, which is attributed to the strong anchor force during electrospinning. The uniform alignment of the director along the fiber is expected to induce a strong mechanical actuation. Upon exposure to UV light, the azobenzene molecules in the surface region of the outmost nanofibers switch from its stable *trans* to *cis* form, causing the parallel alignment nanofiber mat bent toward the direction of the incident light (Figure S7, Supporting Information). Although no significant morphology change was observed on the random alignment mat by field-emission scanning electron microscopy (FESEM), there ought to exist micro/nano pore size changes which could induce the wettability and adhesion changes.

In addition, the surface free energies are also correlated to the topological structure and orientation changes of the nanofibers.[35] Therefore, the rapid and great change of AF on the mats also arises from the reorientation of photoisomerized azobenzenes. Additionally, the order degree of LCs rapidly and greatly decreased upon UV light irradiation on account of the isomerization of azobenzenes and coordinative interaction of LLCPs, which is distinct from other photoresponsive non-LC polymers.[12] In order to investigate the light-induced change of the mesogens orientation, in situ atomic force microscopy (AFM) characterization was performed on the center area of one fiber (Figure 4b). Periodic stripes parallel to each other were seen in the phase images of the nanofiber surface before UV irradiation and their average periodicity is about 4 nm (Figure 4b-I). Upon exposure by UV light (365 nm, 20 mW cm^{-2}) for 2 s, the ordering on the surface was demolished and the surface free energy increased accordingly triggering a transition of the surface free energy and wettability property (Figure 4b-II).[35] Upon exposure by visible light (530 nm, 60 mW cm^{-2}) for 20 s, the ordering of mesogens recovered (Figure 4b-III). Compared
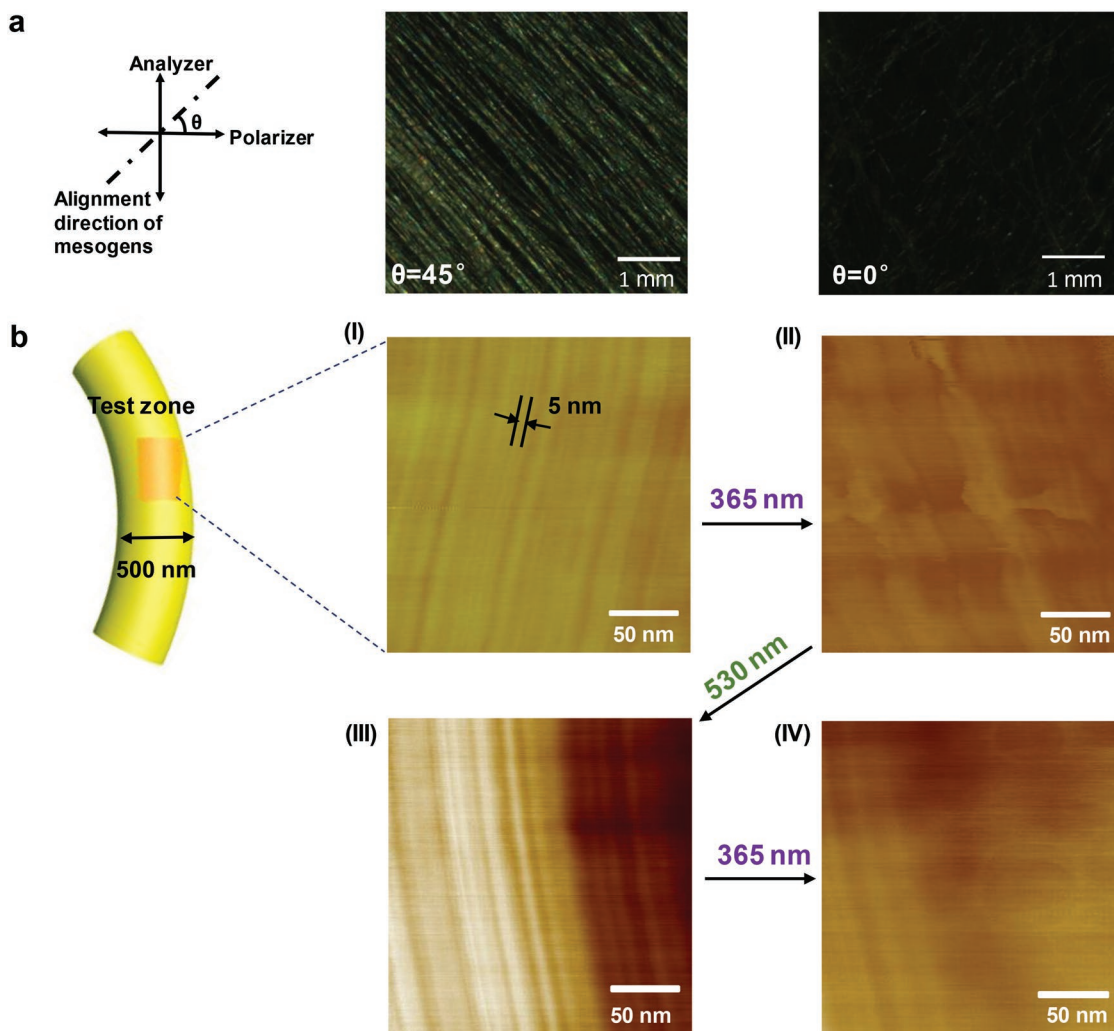
Figure 4. Anisotropic property and nanostructure of nanofibers. a) Polarizing optical microscopy images of nanofibers with parallel alignment. b) The phase images of the nanofiber. The inset region the schematics of a nanofiber indicates the position where AFM maps are recorded. I) The nanofiber before UV exposure. The stripes are parallel to each other and the spacing between two adjacent stripes is about 5 nm. II) The nanofiber after exposure to UV light. The periodic stripes are demolished demonstrating that the order degree of the LCs decreases. III) The nanofiber after visible light irradiation. IV) The nanofiber after the secondary UV irradiation. With the alternating UV–vis irradiation, the order degree of LCs on the LLCP nanofiber surface is alternately varied accordingly. UV light: 365 nm, 20 mW cm^{-2}, 2 s; visible light: 530 nm, 60 mW cm^{-2}, 20 s.

with other types of photoresponsive surfaces, the azobenzene-containing LLCP showed a much larger and faster change of wettability behavior, which is beneficial to develop more intelligent and amusing devices.

3. Conclusion

We have presented for the first time the fabrication of photoresponsive LLCP nanofibers with hierarchical structures by electrospinning of high-molecular-weight photoresponsive LLCP and successfully prepared large-area superhydrophobic LLCP mats with phototunable wettabilities. Compared to the previous reported photoresponsive polymer surfaces, our superhydrophobic LCP mats exhibit fast and reversible superhydrophobic adhesion changes upon the alternated irradiation of UV–vis light while maintaining the superhydrophobicity. With these

photoresponsive mats, directed pinning the moving water droplets has been realized remotely at the desired position. We anticipate that the novel photoresponsive LLCP mats could provide an ideal platform to achieve the active manipulation of discrete droplets on an open surface and the process of directed pinning of moving water droplets will inspire the designs and facilitate applications of novel microfluidic devices.

4. Experimental Section

Electrospinning: For the preparation of electrospinning solutions, LLCP was dissolved in CH$_2$Cl$_2$ with the concentration of 1, 3, and 5 wt% by stirring for 1 h and ultrasonic treating for 10 min. The electrospinning process was performed using a home-made setup including a high voltage power supply, a syringe with stainless steel blunt-ended needle, and a rectangular metal collector. The working distances between the needle tip and collector were set 20 cm. The appropriate voltage was

varied for the purpose of obtaining requirement-meeting fiber films. The Mats I–III were collected on iron plat for 30 min and then dried in room temperature for 2 h to remove remaining solvents.

Measurements and Characterization: The surface morphology of the electrospun nanofibers was examined by FESEM (Zeiss, Ultra 55). The UV–vis spectra of diluted solutions of LLCP was recorded by UV–vis–near infrared (NIR) spectrophotometer (Pekin Elmer, Lambda650). The number molecular weight of the LLCP was performed in tetrahydrofuran by gel permeation chromatography (Agilent, 1260). The mesomorphic properties of the parallel aligned mats were studied by optical polarizing microscopy (POM) (Leica, DM2500P). AFM tapping mode images were acquired using an atomic force microscope (Bruker, Multimode 8). 2D WAXD experiments of the LLCP mats were conducted on a Bruker D8 Discover diffractometer with a 2D detector of general area detector diffraction system (GADDS) in the transmission mode. The X-ray sources (Cu Kα, $\lambda = 0.154$ nm) were provided by 3 kW ceramic tubes and the peak positions were calibrated with silicon powder ($2\theta > 15°$) and silver behenate ($2\theta < 10°$). The background scattering was recorded and subtracted from the sample patterns. AF measurements were performed on Dataphysics DCAT11. The CAs and SAs were measured by means of a contact angle system (DataPhysics, OCA20). The average CA and SA values were obtained by measuring the same sample at least in five different positions. The light-controlled experiments were performed using 365 nm light-emitting diode (LED) UV light (Omron, ZUV-C30H) and 530 nm LED visible light (CCS, HLV-24GR-3W).

Supporting Information

Supporting Information is available from the Wiley Online Library or from the author.

Acknowledgements

Conflict of Interest

The authors declare no conflict of interest.

Keywords

[1] P. F. Hao, C. J. Lv, X. W. Zhang, Z. H. Yao, F. He, *Chem. Eng. Sci.* **2011**, *66*, 2118.

[2] J. Atencia, D. J. Beebe, *Nature* **2005**, *437*, 648.

[3] D. Mannetje, S. Ghosh, R. Lagraauw, S. Otten, A. Pit, C. Berendsen, J. Zeegers, D. Ende, F. Mugele, *Nat. Commun.* **2014**, *5*, 3559.

[4] Y. Huang, B. B. Stogin, N. Sun, J. Wang, S. K. Yang, T. Wong, *Adv. Mater.* **2017**, *29*, 1604641.

[5] G. Y. Huang, M. X. Li, Q. Z. Yang, Y. H. Li, H. Liu, H. Yang, F. Xu, *ACS Appl. Mater. Interfaces* **2017**, *9*, 1155.

[6] Y. Y Liu, B. Xu, S. T. Sun, J. Wei, L. M. Wu, Y. L. Yu, *Adv. Mater.* **2017**, *29*, 1604792.

[7] J. Lv, Y. Y Liu, J. Wei, E. Q. Chen, L Qin, Y. L. Yu, *Nature* **2016**, *537*, 179.

[8] Y. Li, L. L. He, X. F. Zhang, N. Zhang, D. L. Tian, *Adv. Mater.* **2017**, *29*, 1703802.

[9] K. Ichimura, S. K. Oh, M. Nakagawa, *Science* **2000**, *288*, 1624.

[10] C. L. Gao, L. Wang, Y. C. Lin, J. T. Li, Y. F. Liu, X. Li, S. L. Feng, Y. M. Zheng, *Adv. Funct. Mater.* **2018**, *28*, 1803072.

[11] J. Wang, W. Gao, H. Zhang, M. H. Zou, Y. P. Chen, Y. J. Zhao, *Sci. Adv.* **2018**, *4*, 7392.

[12] S. T. Wang, Y. L. Song, L. Jiang, *J. Photochem. Photobiol., C* **2007**, *8*, 18.

[13] M. Chen, F. Besenbacher, *ACS Nano* **2011**, *5*, 1549.

[14] C. Li, F. Cheng, J. Lv, Y. Zhao, M. Liu, L. Jiang, Y. L. Yu, *Soft Matter* **2012**, *8*, 3730.

[15] Z. Yan, X. Ji, W. Wu, J. Wei, Y. Yu, *Macromol. Rapid Commun.* **2012**, *33*, 1362.

[16] C. Li, Y. Zhang, J. Ju, F. Cheng, M. Liu, L. Jiang, Y. Yu, *Adv. Funct. Mater.* **2012**, *22*, 760.

[17] Y. Y. Zhan, J. Q. Zhao, W. D. Liu, B. Yang, Y. L. Yu, J. Wei, *ACS Appl. Mater. Interfaces* **2015**, *7*, 25522.

[18] Y. Y Liu, W. Wu, J. Wei, Y. L. Yu, *ACS Appl. Mater. Interfaces* **2017**, *9*, 782.

[19] J. Wei, Y. L. Yu, *Soft Matter* **2012**, *8*, 8050.

[20] W. Wang, X. M. Sun, W. Wu, H. S. Peng, Y. L. Yu, *Angew. Chem., Int. Ed.* **2012**, *51*, 4644.

[21] Z. Jiang, M. Xu, F. Y. Li, Y. L. Yu, *J. Am. Chem. Soc.* **2013**, *135*, 16446.

[22] D. Q. Liu, D. J. Broer, *Angew. Chem., Int. Ed.* **2014**, *53*, 4542.

[23] T. Ube, T. Ikeda, *Angew. Chem., Int. Ed.* **2014**, *53*, 10253.

[24] T. White, D. Broer, *Nat. Mater.* **2015**, *14*, 1087.

[25] X. Qing, Y. Y. Liu, J. Wei, R. Zheng, C. Y. Zhu, Y. L. Yu, *Adv. Opt. Mater.* **2019**, *7*, 1801494.

[26] X. Qing, J. -a. Lv, Y. L. Yu, *Acta Polym. Sin.* **2017**, *11*, 1679.

[27] N. Nuraje, W. S. Khan, Y. Lei, M. Ceylanb, R. Asmatulu, *J. Mater. Chem. A* **2013**, *1*, 1929.

[28] E. Enz, J. Lagerwall, *J. Mater. Chem.* **2010**, *20*, 6866.

[29] J. Lagerwall, J. T. McCann, E. Formo, G. Scalia, Y. Xia, *Chem. Commun.* **2008**, 5420.

[30] H. Ling, E. Eva, G. Scalia, J. Lagerwall, *Mol. Cryst. Liq. Cryst.* **2011**, *549*, 69.

[31] S. Krause, R. Dersch, J. H. Wendorff, H. Finkelmann, *Macromol. Rapid Commun.* **2007**, *28*, 2062.

[32] A. C. Trindade, J. P. Canejo, P. I. C. Teixeira, P. Patrício, M. H. Godinho, *Macromol. Rapid Commun.* **2013**, *34*, 42.

[33] A. Sharma, J. Lagerwall, *Materials* **2018**, *11*, 393.

[34] M. H. Ran, C. X. Yang, Y. Fang, K. K. Zhao, Y. Q. Ruan, J. Wu, H. Yang, Y. F. Liu, *J. Phys. Chem. C* **2012**, *116*, 8449.

[35] T. Seki, H. Sekizawa, S. Morino, K. Ichimura, *J. Phys. Chem. B* **1998**, *102*, 5313.